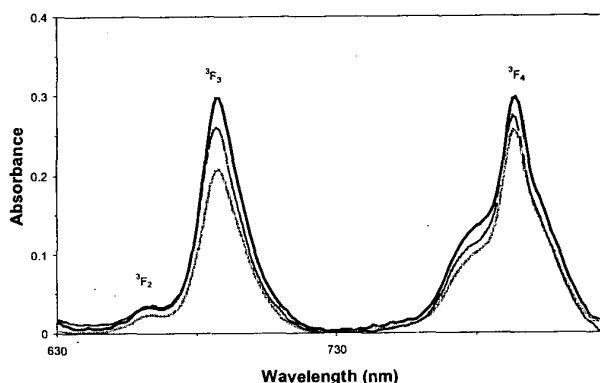
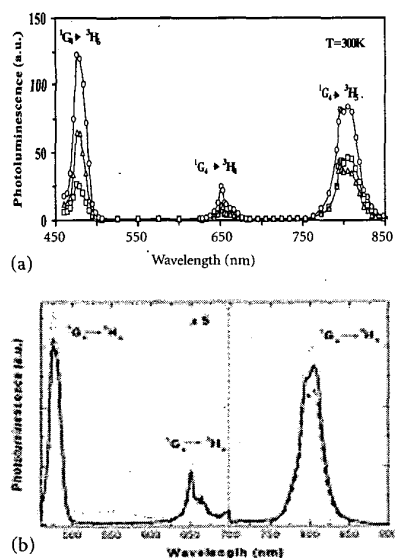


CTuK55 Table 1. Stimulated emission cross-sections,  $\sigma_{se}$ , for the emissions of  $Tm^{3+}$  in  $(1-x)TeO_2 - (x)WO_3$  glass observed upon 457.9 nm laser light excitation

Glass Composition (mol %)			$\sigma_{se}$ ( $\times 10^{-21}$ cm <sup>2</sup> )					
			$^1G_4 \rightarrow ^3H_6$		$^1G_4 \rightarrow ^3H_4$		$^1G_4 \rightarrow ^3H_5$	
TeO <sub>2</sub>	WO <sub>3</sub>	Tm <sub>2</sub> O <sub>3</sub>	T = 300 K	T = 10 K	T = 300 K	T = 10 K	T = 300 K	T = 10 K
85	15	1	3.9	4.2	5.8	7.5	7.5	23.1
75	25	1	4.3	7.3	2.4	3.8	1.3	22.8
70	30	1	4.5	7.9	2.1	8.2	1.2	22.7



CTuK55 Fig. 1. Variation of the  $Tm^{3+}$  absorbance with the modifier in the range of pumping wavelength 630 nm–800 nm (—: 0.3 mol.  $CdCl_2$ , ---: 0.3 mol.  $LiCl$  and ···: 0.3 mol.  $WO_3$ ).



CTuK55 Fig. 2. a) Effect of composition on the luminescence bands (excitation was made with a laser tuned at 457.9 nm)  $\square$ : 0.15 mol.,  $\Delta$ : 0.25 mol. and,  $\circ$ : 0.30 mol.  $WO_3$  content. b) Effect of composition on the spectral profiles of the luminescence bands (excitation was into the  $^1G_4$  level of  $Tm^{3+}$  ion with a laser tuned at 457.9 nm)  $\square$ : 0.15 mol.,  $\Delta$ : 0.25 mol. and,  $\circ$ : 0.30 mol.  $CdCl_2$  content in  $TeO_2$ - $CdCl_2$  glass.

$1.95 \times 10^{-20}$  cm<sup>2</sup> for the  $CdCl_2$ ,  $LiCl$  and  $WO_3$  modifiers, respectively.

Effect of the  $WO_3$  (presented in Fig. 2a) and  $CdCl_2$  (presented in Fig. 2b) content on the luminescence band structure and the intensities at room temperature are also very similar.

For both modifiers, integrated intensity of the emissions due to the  $^1G_4 \rightarrow ^3H_6$  transition first shows a decrease and then an increase while the integrated intensity of the emissions due to the  $^1G_4 \rightarrow ^3H_4$  and  $^1G_4 \rightarrow ^3H_5$  transitions decrease with increasing amount of modifier.

Stimulated emission cross-section at the peak wavelength of the emission bands,  $\sigma(\lambda_p)$ , was determined using the formula given in ref. [5] and, the results obtained for the  $TeO_2$ - $WO_3$  glass are presented in Table 1.

From our data, it can be concluded that  $Tm^{3+}$  doped binary tellurite glasses are promising materials for the infra-red amplifiers as well as the blue up-conversion lasers when the wavelength of the pumping light is chosen as 650 nm.

#### References

1. S. Tanabe, "Optical transitions of rare earth ions for amplifiers: how the local structure works in glass", *J. Non-Cryst. Solids* 259, 1–9 (1999).
2. K. Mizato, D.F. de Sousa, A. Delben, J.R. Delben, S.L. de Oliveira, L.A.O. Nunes, "Up-conversion mechanisms in  $Tm^{3+}$  doped lead fluoroindogallate glasses", *J. Non-cryst. Solids* 273, 246–251 (2000).
3. B.R. Judd, "Optical Absorption Intensities of Rare-Earth Ions", *Phys. Rev.* 127, 750–761 (1962).

4. G.S. Ofelt, "Intensities of crystal spectra of rare-earth ions", *J. Chem. Phys.* 37, 511–520 (1962).
5. W.F. Krupke, "Induced emission cross-sections in neodymium doped glasses", *IEEE J. Quant. Electron.*, QR-10, 450–457 (1974).

#### CTuK56

1:00 pm

#### Liquid Phase Epitaxy, Spectroscopic Investigation, and Broadband Emission of $BaSO_4:Mn^{6+}$ Layers

D. Ehrentauf, and M. Pollnau, *Institute of Applied Optics, Department of Microtechnique, Swiss Federal Institute of Technology, CH-1015 Lausanne, Switzerland*

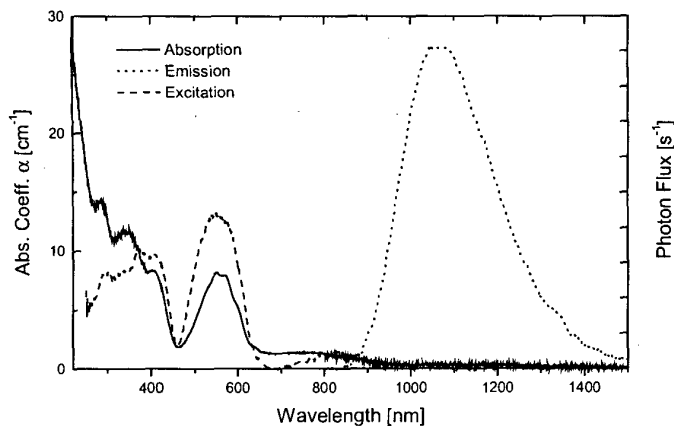
S. Kück, *Institute of Laser-Physics, University of Hamburg, Jungiusstrasse 9a, D-20355 Hamburg, Germany*

Because of the strong electron-phonon coupling of the emitting 3d orbitals in transition-metal (TM) 3d systems exhibit luminescence with typically several hundred nm of spectral bandwidth. TM-ion-doped materials are, therefore, of high interest for applications as tunable and short-pulse lasers. Whereas many TM-ion-doped systems suffer from excited-state absorption (ESA), systems with a  $d^1$  electron configuration possess only one excited 3d level and ESA into higher-lying 3d levels is impossible (however, ESA can occur owing to transitions into the conduction band and conduction-band-related energy levels). One of these  $d^1$  systems, Ti:sapphire has become the most successful tunable and short-pulse laser system to date.

$Mn^{6+}$  is a promising ion for a tunable laser system. Recently, near-infrared emission from  $Mn^{6+}$  was observed in several host lattices.<sup>1,2</sup> In  $BaSO_4$ , the room-temperature stimulated-emission cross section is larger than the excited-state-absorption cross section in the spectral range 920–1600 nm,<sup>3</sup> i.e., as a laser material  $BaSO_4:Mn^{6+}$  can offer a broad tuning range. However, the size and crystalline quality of the crystals were not sufficient for laser experiments.

Here we report on the first epitaxial growth of  $Mn^{6+}$ -doped  $BaSO_4$  layers. Growth techniques such as the melt growth that work at higher temperatures fail, because  $BaSO_4$  has a phase transition at 1090°C<sup>4</sup> and a melting point does not exist due to the thermal decomposition of  $BaSO_4$  at 1590°C. We grew  $BaSO_4$  bulk crystals of  $10 \times 6 \times 4$  mm<sup>3</sup> in size at 650–480°C by the flux method from a  $LiCl$  solvent. Due to the high supersaturation necessary for the formation of  $BaSO_4$  seed crystals, inclusions were incorporated into the crystal. Therefore, we grew undoped  $BaSO_4$  on the flux-grown  $BaSO_4$  crystals by use of liquid phase epitaxy (LPE). We used the same solid composition as for the LPE of  $BaSO_4:Mn^{6+}$  active layers described later. Since LPE works closer to the thermodynamic equilibrium, the surface inclusions of the flux-grown substrates were dissolved until equilibrium faces remained. This procedure resulted in undoped  $BaSO_4$  layers with surfaces flat enough for the subsequent growth of high-quality active layers.

Chemical instability of a desired valence state of the active dopant can pose a major problem on the fabrication of an optically active material. The manganese ion exists in all oxidation states from



CTuK56 Fig. 1. Absorption, emission, and excitation spectra of a  $\text{BaSO}_4:\text{Mn}^{6+}$  layer. The absorption coefficient is relevant to the whole sample of 2-mm thickness.

$\text{Mn}^{2+}$  to  $\text{Mn}^{7+}$ . The stabilities of the different valence states depend on growth temperature and chemical character of the solution. The  $\text{Mn}^{6+}$  ions tend to reduce to  $\text{Mn}^{5+}$  at  $T \approx 620^\circ\text{C}$ .<sup>1</sup> We used a CsCl-KCl-NaCl solvent<sup>5</sup> for the LPE of  $\text{BaSO}_4:\text{Mn}^{6+}$ . This solvent has a low solidification temperature of  $480^\circ\text{C}$  and the growth process could be performed at temperatures well below  $620^\circ\text{C}$ . Chemical reduction of the Mn ions was avoided and only  $\text{Mn}^{6+}$  was incorporated into our layers. Other chloridic solvents are less suitable owing to higher melting points or chemical reactions with the solute.<sup>5</sup>

The active layers were grown under ambient atmosphere in the temperature region  $550\text{--}508^\circ\text{C}$ . The nominal  $\text{Mn}^{6+}$  concentration was up to 0.67 mol%. High quality, lack of large-size inclusions, and low defect concentration were achieved. We grew layers with thickness of up to  $175\ \mu\text{m}$  at growth velocities of approximately  $3\ \mu\text{m h}^{-1}$ . The layer thickness is controllable with sub- $\mu\text{m}$  precision. Besides the possibility to grow bulk samples, these values enable us to fabricate planar sandwich waveguides of desired thickness.

The  $\text{Mn}^{6+}$ -doped  $\text{BaSO}_4$  layers were investigated spectroscopically by absorption, emission, and luminescence-excitation measurements at room temperature. The absorption and luminescence-excitation spectra of Fig. 1 are similar to each other. The  $\text{Mn}^{6+}$  absorption bands are assigned according to  ${}^3\text{E} \rightarrow {}^2\text{T}_2$  at  $700\text{--}900\ \text{nm}$  and a ligand-to-metal charge-transfer band at  $500\text{--}650\ \text{nm}$ . Excitation into these bands leads to broadband  $\text{Mn}^{6+}$  emission between  $850$  and  $1600\ \text{nm}$ . After further optimization of the growth process and preparation of suitable  $\text{BaSO}_4:\text{Mn}^{6+}$  samples, we will investigate the potential of  $\text{BaSO}_4:\text{Mn}^{6+}$  for tunable near-infrared laser emission.

1. T.C. Brunold and H.U. Güdel, *Inorg. Chem.* **36**, 1946 (1997).
2. T.C. Brunold and H.U. Güdel, *Chem. Phys. Lett.* **249**, 77 (1996).
3. T.C. Brunold, H.U. Güdel, S. Kück, and G. Huber, *J. Opt. Soc. Am. B* **14**, 2373 (1997).
4. H. Sawada and Y. Takeuchi, *Z. Krist.* **191**, 161 (1990).
5. D. Ehrentraut and M. Pollnau, "Flux growth of baryte-type  $\text{BaSO}_4$  from chloridic alkaline

metal solvents", *J. Cryst. Growth*, accepted for publication.

#### CTuK57

1:00 pm

#### Thermal Poling Studies in Phosphate Glasses

P. Thamboon and D.M. Krol, Department of Applied Science, University of California at Davis, Davis, CA 95616, Lawrence Livermore National Laboratory, Livermore, CA, 94550, Email: thamboon1@lml.gov.dmkrol@ucdavis.edu

The objective of our research is to introduce a second-order optical nonlinearity ( $\chi^{(2)}$ ) in phosphate glasses via the thermal poling technique, in order to enable the fabrication of integrated waveguide frequency-doubled lasers.

Second order optical nonlinearities ( $\chi^{(2)}$ ) were induced in commercial phosphate glasses (Schott, IOG-1) and in self-prepared lanthanum phosphate (20%  $\text{La}_2\text{O}_3$ , 80%  $\text{P}_2\text{O}_5$ ) glasses by the thermal poling technique.<sup>1</sup> The Al coated glass samples were placed in between stainless steel electrodes and were subjected to high DC fields and elevated temperatures for a certain poling

time before cooling them down to room temperature and removing the field. DC fields ranging from 1 to 5 kV and temperatures ranging from 100 to  $500^\circ\text{C}$  were used in the process. Due to a high content of Na ions in IOG-1 samples, lower applied DC fields and temperature ranges were preferable to prevent overshoot current through the poled samples.

The induced second order nonlinearities were measured via second harmonic generation using a fundamental beam from a 1064 nm mode-locked Nd:YAG laser. The nonlinear regions were characterized using the Maker-Fringe technique, in which the second harmonic signals are measured as a function of incident angle of the fundamental beam. A schematic diagram of the experimental set-up is shown in fig. 1.

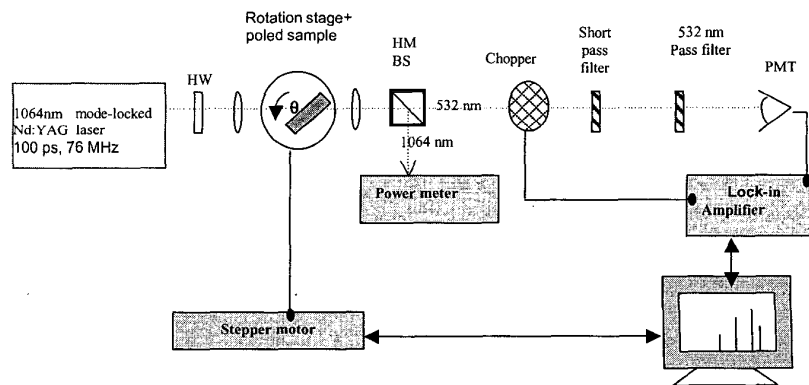
Typical Maker fringe patterns from IOG-1 samples are shown in fig. 2. The results show that the signal does not decrease over a 3-month period indicating that the induced  $\chi^{(2)}$  is permanent at room temperature. Furthermore the observed fringe pattern shows a fast oscillation superimposed on a slow modulation, thereby revealing two nonlinear regions, a surface and a bulk contribution.<sup>2</sup> Detailed information about the magnitude and spatial profile of the induced nonlinearity is obtained by fitting the observed Maker fringe patterns to the following expression:

$$P_{2\omega}(\theta) \propto \left| P_{\omega} d_{33}(z) \sin\theta \exp(i\Delta kz/\cos\theta) dz \right|^2,$$

where  $z$  is along the poling direction and  $\Delta k$  is the phase-mismatch for SHG in phosphate glasses at 1064 nm.

The signals from lanthanum phosphate samples were only observed at higher applied DC fields ( $>3\ \text{kV}$ ) and higher temperatures ( $>300^\circ\text{C}$ ). The dependence of the induced  $\chi^{(2)}$  profile on applied poling fields, temperatures and poling time for both types of glasses will be discussed. A microscopic model that can explain the observed behavior will also be proposed.

This work was performed under the auspices of the U.S. Department of Energy by University of California Lawrence Livermore National Laboratory, through the Institute for Laser Science and Applications, under contract No. W-7405-Eng-48. The authors acknowledge financial support from NSF grant ECS 0083087.



CTuK57 Fig. 1. The Maker fringe experimental set-up. HW: Half Waveplate, L: lens, HM BS: Harmonic Beamsplitter, PMT: photomultiplier tube.